Available online at www.sciencedirect.com

ScienceDirect

Mendeleev Commun., 2024, **34**, 569–571

Mendeleev Communications

Enhanced performance of bimetallic catalysts based on copper phyllosilicate in the hydrogenation of dimethyl oxalate to ethylene glycol

Anastasiya A. Shesterkina,*[a] Victoria S. Zhuravleva,[a,b] Kristina E. Kartavova,[a] Anna A. Strekalova,[b] Kseniia V. Vikanova[a] and Alexander L. Kustov[a]

[a] *Department of Chemistry, M. V. Lomonosov Moscow State University, 119991 Moscow, Russian Federation. E-mail: anastasiia.strelkova@mail.ru*

[b] *N. D. Zelinsky Institute of Organic Chemistry, Russian Academy of Sciences, 119991 Moscow, Russian Federation*

DOI: 10.1016/j.mencom.2024.06.033

The effect of the second metal (Pt, Pd, Ni and Fe) on the activity of copper phyllosilicate-based catalysts was investigated in the selective hydrogenation of dimethyl oxalate to ethylene glycol at 160–200 °C. The prepared catalysts were characterized by XRD, DRIFTS-CO and TEM methods. The conversion achieved over 10Fe/10Cu-PhySi catalyst was 68 % at 200 °C; at the same time, the full conversion with selectivity 98% was obtained at the temperature of 180 °C over a bimetallic 1Pt/Cu-PhySi catalyst.

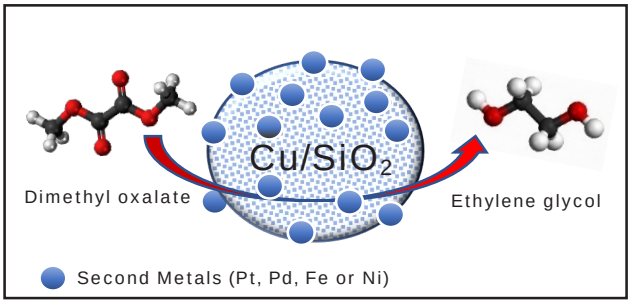

Keywords: dimethyl oxalate, ethylene glycol, ester hydrogenation, copper phyllosilicate, bimetallic catalyst, copper catalyst.

Ethylene glycol (EG) is one of the main starting materials for the production of polyethylene terephthalate (81% of total consumption). It is also widely used as a solvent and media component in electrolytic capacitors and hydraulic brake fluids.[1–3] The chemical industry produced 42 million tons of EG in 2020. According to analysts, global production capacity of ethylene glycol increased from approximately 30.24 million tons in 2014 to almost 57 million metric tons in 2022.[4]

There are several ways to obtain ethylene glycol. Most of EG is manufactured by oxidation of ethylene following by its subsequent hydration. However, production is limited by crude oil reserves and strict environmental regulations. At the same time, EG can be produced from syngas which can be obtained from renewable sources such as natural gas and biomass. Therefore, the method of EG production *via* the use of bio-available compounds is much more economically and environmentally promising. In a one-step synthesis, CO directly reacts with H_2 forming EG, which is technologically efficient but thermodynamically unfavorable.[5] In this regard, an indirect method is more preferable, it includes the reaction of the combination of carbon monoxide with the formation of dimethyl oxalate (DMO) and its subsequent hydrogenation that yields the target product, ethylene glycol.[6,7]

The most suitable catalysts for ester hydrogenation are copper-based catalysts, inasmuch as copper compounds are effective for the hydrogenation of C=O carbonyl groups, but are inactive for the hydrogenolysis of C–C bond cleavage.[8–11] SiO_2 is often used as a support due to the presence of weakly pronounced acid-base properties.[12] The main challenge here is EG selectivity, whereas in the hydrogenation of DMO at temperatures below 190 °C a large amount of a by-product, methyl glycolate, is observed, while the carrying out of the reaction at temperatures above 210 °C results in the EG reduction to ethanol.[13]

Among the variety of different copper-based catalytic systems, phyllosilicates hold a special place; unlike traditional SiO_2-based copper oxide, phyllosilicate (PhySi) has an improved thermal stability, higher dispersion of copper particles and larger specific surface area due to its layered structure.[14,15] A. Yin *et al.*[16] reported that the 10Cu/HMS (SiO_2) catalyst with hydrosilicate structure demonstrated the 87 % conversion in DMO hydrogenation with a 75 % EG selectivity at 250 °C, 2.5 MPa H_2 pressure, H_2/DMO = 120 mol mol^{-1} and DMO LSV = 0.20 h^{-1}. It should be noted that on the copper oxide-based catalyst prepared by the impregnation method DMO conversion was only 41% with 68% EG selectivity. In our previous work[17] we have demonstrated that copper phyllosilicate are quite effective and promising systems for selective hydrogenation of unsaturated compounds. Thus, the aim of this work has been to investigate the catalytic properties of copper phyllosilicate with different Cu content and the effect of the second metal (Pd, Pt, Ni and Cu) in bimetallic catalysts on their activity in the DMO conversion to EG.

The synthesis of the bimetallic copper phyllosilicate-based catalysts is described.[†] All the synthesized catalysts proved to be catalytically active under the reaction conditions (160–200 °C,

[†] The 5–10% Cu/SiO_2 catalysts with the chrysocolla structure (*x*Cu-PhySi) were prepared by deposition–precipitation of $Cu(NO_3)_2$ on the SiO_2 support *via* thermal hydrolysis of urea (DPU-method). A detailed synthesis of monometallic copper samples is described in our previous work.[14] Supported bimetallic catalysts containing 1 wt% of noble (Pt or Pd) and 10 wt% of non-noble (Ni or Fe) metals were synthesized by incipient wetness impregnation of the *x*Cu-PhySi sample with an aqueous solution of metal precursors. Commercial chemicals, H_2PtCl_6, H_2PdCl_4, $Ni(NO_3)_2{\cdot}6H_2O$, $Cu(NO_3)_2{\cdot}3H_2O$ and $Fe(NO_3)_3$, were used as metal precursors. Then impregnated samples were dried at 110 °C for 12 h and calcined in air at 300 °C for 3 h. Their phase composition was identified by X-ray diffraction (XRD) method using an ARL X′TRA diffractometer

3.0 MPa), however, the activity of Cu-PhySi catalysts was relatively low and increased with rising Cu content (Figure 1). The highest DMO conversion (56%) was obtained in the presence of 10Cu-PhySi sample at a temperature of 200 °C. Therefore, further catalytic studies were carried out on bimetallic catalysts with the copper loading of 10 wt%.

The modification of monometallic 10Cu-PhySi samples with additives of both noble (Pt and Pd) and non-noble (Fe and Ni) metals made it possible to enhance the efficiency of the catalysts. Thus, doping of a monometallic 10Cu-PhySi catalyst by 1 wt% Pd or Pt will increase the DMO conversion from 20 to 60–80% at the temperature of 160 °C. The use of Fe and Ni as a promoter allowed us to increase DMO conversion twice as compared with a monometallic sample. With the temperature rise, the increase of DMO conversion over almost all catalysts was observed. The optimal reaction conditions for the catalysts containing the noble metals (1Pd/10Cu-PhySi and 1Pt/10Cu-PhySi) were 180 °C and $P(H_2)$ = 3 MPa. The use of the samples with non-precious metals, 10Fe/10Cu-PhySi and 10Ni/10Cu-PhySi, required a higher temperature (up to 200 °C) for this reaction.

Figure 2 demonstrates the EG selectivity over the mono- and bimetallic 10Cu-PhySi catalysts at optimal temperature of 180 °C. It is clearly seen that for all prepared catalysts the EG selectivity exceeded 93 %. The by-product in all cases was methyl glycolate, the ethanol formation was not observed.

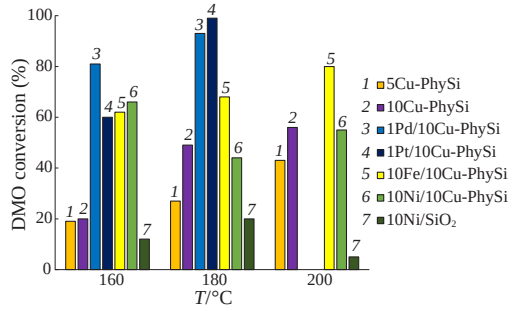

Figure 1 The temperature effect on DMO conversion over the Cu-containing catalysts.

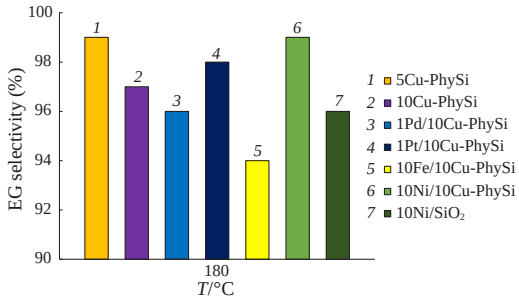

Figure 2 EG selectivity at the reaction temperature of 180 °C.

(Thermo Fisher Scientific). The morphological properties of the catalysts were investigated by TEM method using a JEOL JEM-2100 transmission electron microscope. Diffuse-reflectance IR spectra were measured at room temperature on a NICOLET Protege 460 spectrometer in the 6000–400 cm^{-1} range with a resolution of 4 cm^{-1}.

Before the experiments, catalysts (fraction of 0.25–0.5 mm) were reduced in a hydrogen flow at 250 °C for 2 h. The DMO hydrogenation to EG was investigated in a flow-type reactor in temperature range of 160–200 °C and H_2 pressure of 3.0 MPa. The catalyst loading was 100 mg, the volumetric feed rate of the feedstock (raw material) (10 wt% dimethyl oxalate in methanol) was v = 0.06 ml min^{-1}, the hydrogen feed rate was v = 30 ml min^{-1} and the molar ratio of H_2 : feedstock (raw material) was 30 : 1. The reaction products were analyzed on a Kristall-5000 gas chromatograph on a column with 100% dimethylpolysiloxane (ZB-1, length 60 m, diameter 0.32 mm) with a flame ionization detector. The activity of the catalysts was evaluated by the DMO conversion and the reaction products.

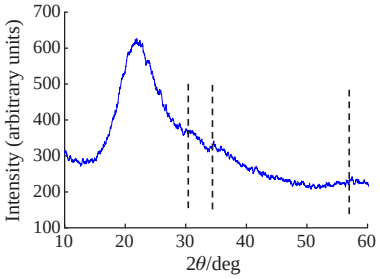

Figure 3 XRD profile of 10Cu-PhySi catalyst.

The phase composition of the catalysts was estimated using the XRD analysis and the electronic state of the metals was studied by DRIFTS-CO method. On XRD profile (see Figure 3) of the 10Cu-PhySi sample, broadened reflexes at 2θ values of 30.5, 35.8 and 56.9° are distinguishable, which agree with the standard reflexes of the (132), (023) and (360) chrysocolla planes (ICDD # 27-0188).[18–20] This indicates that copper nanoparticles are finely dispersed over the surface of the carrier. No signals from the Pt and Pd phases were detected on the XRD profiles of bimetallic catalysts, probably because of the noble metals low content.

The DRIFTS-CO spectra (Figure 4) recorded for the bimetallic 10Fe/10Cu-PhySi catalyst showed a low-intensity band at 2360 cm^{-1} corresponding to the Fe^{2+}–CO_2 complex

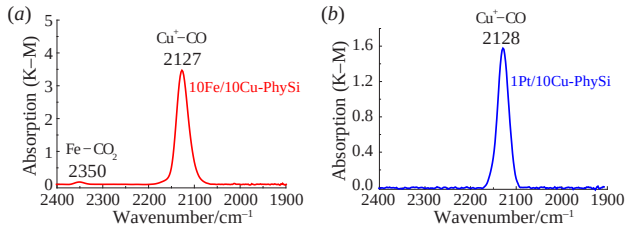

Figure 4 DRIFTS-CO study of (*a*) 10Fe/10Cu-PhySi and (*b*) 1Pt/10Cu-PhySi catalysts.

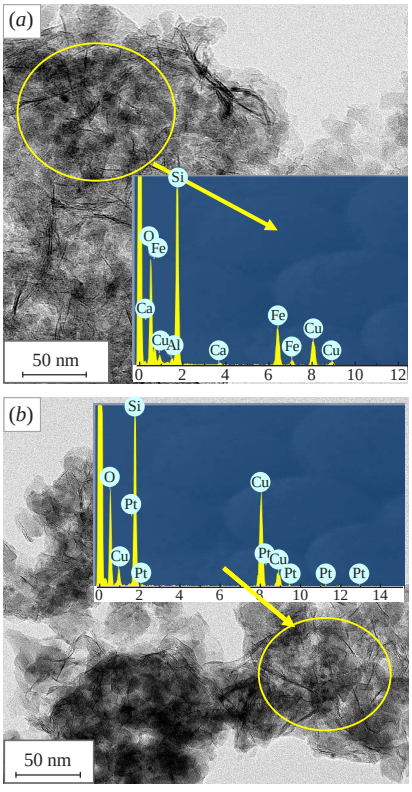

Figure 5 TEM images of (*a*) 10Fe/10Cu-PhySi and (*b*) 1Pt/10Cu-PhySi catalysts.

formed as a result of Fe^{3+} reduction by CO[21] and an intense line at 2127–2128 cm^{-1} that can be assigned to the stretching vibrations of CO molecules adsorbed on Cu^{+} cations.[22] The same band was observed in the 1Pt/10Cu-PhySi spectra.

TEM-EDX analysis was carried out to examine the distribution of supported metals (Pt and Fe) over the surface of the 10Cu-PhySi support (see Figure 5). The micrographs of both bimetallic catalysts show the 'fibrous' microstructure of the samples characteristic for the phyllosilicate materials. In addition, microphotographs of both catalysts show uniformly dispersed metallic phases represented by spherical nanoparticles. The average calculated size of spherical particles in the 1Pt/10Cu-PhySi sample is 5 nm. EDX analysis of this sample indicates the presence of Pt and Cu in the sample. In case of the 10Fe/10Cu-PhySi catalyst, the size of nanoparticles is much larger and amounts to 9 nm. The results of the EDX analysis allows us to conclude that these nanoparticles belong to the supported iron phase.

Thus, the nature of the second metal affects a synergistic interaction with the copper phyllosilicate phase, significantly increasing the activity and selectivity of the catalyst in the hydrogenation of DMO to EG. Adding 1 wt% of Pt to the copper-based catalytic system made it possible to increase the conversion to 99% and to reach the 98% EG selectivity. However, the replacement of platinum with more affordable and cheaper metal, iron, allowed one to maintain almost the same selectivity level (94%) with a slight decrease of DMO conversion to 68%.

This research was supported by Russian Science Foundation, grant no. 23-73-01034, https://rscf.ru/en/project/23-73-01034/.

References

1 L. Li, D. Ren, J. Fu, Y. Liu, F. Jin and Z. Huo, *J. Energy Chem.*, 2016, **25**, 507.
2 J. Yang, L. Lin, P. Zhang, R. Ye, Y. Wang, Y. Qin, Z. Zhou and Y.-G. Yao, *Ind. Eng. Chem. Res*., 2023, **62**, 14866.
3 P. Ai, H. Jin, J. Li, X. Wang and W. Huang, *Chin. J. Chem. Eng*., 2023, **60**, 186.
4 *Statista: Ethylene glycol production capacity globally 2014–2022*, https://www.statista.com/statistics/1067418/global-ethylene-glycol-production-capacity/ accessed January 26th, 2024.
5 H. Yue, Y. Zhao, X. Ma and J. Gong, *Chem. Soc. Rev.*, 2012, **41**, 4218.
6 C.-W. Jiang, Z.-W. Zheng, Y.-P. Zhu and Z.-H. Luo, *Chem. Eng. Res. Des*., 2012, **90**, 915.
7 B.-Y. Yu and I.-L. Chien, *Chem. Eng. Res. Des.*, 2017, **121**, 173.
8 A. A. Strekalova, A. A. Shesterkina, L.M. Kustov, *Catal. Sci. Technol.*, 2021, **11**, 7229.
9 R.-P. Ye, L. Lin, L.-C. Wang, D. Ding, Z. Zhou, P. Pan, Z. Xu, J. Liu, H. Adidharma, M. Radosz, M. Fan and Y.-G. Yao, *ACS Catal.*, 2020, **10**, 4465.
10 X.-P. Kong, X.-M. You, P.-H. Yuan, Y.-H. Wu, R.-H. Wang and J.-G. Chen, *J. Fuel Chem. Technol.*, 2023, **51**, 794.
11 A. A. Shesterkina, A. A. Strekalova, E. V. Shuvalova, G. I. Kapustin, O. P. Tkachenko and L. M. Kustov, *Mendeleev Commun.*, 2022, **32**, 672.
12 D. S. Brands, E. K. Poels and A. Bliek, *Appl. Catal., A*, 1999, **184**, 279.
13 J. Gong, H. Yue, Y. Zhao, S. Zhao, L. Zhao, J. Lv, S. Wang and X. Ma, *J. Am. Chem. Soc.*, 2012, **134**, 13922.
14 A. A. Shesterkina, K. V. Vikanova, V. S. Zhuravleva, A. L. Kustov, N. A. Davshan, I. V. Mishin, A. A. Strekalova and L. M. Kustov, *Mol. Catal.*, 2023, **547**, 113341.
15 X. Dong, X. Ma, H. Xu and Q. Ge, *Catal. Sci. Technol.*, 2016, **6**, 4151.
16 A. Yin, X. Guo, W.-L. Dai, H. Li and K. Fan, *Appl. Catal., A*, 2008, **349**, 91.
17 A. Shesterkina, K. Vikanova, E. Kostyukhin, A. Strekalova, E. Shuvalova, G. Kapustin and T. Salmi, *Molecules*, 2022, **27**, 988.
18 T. Toupance, M. Kermarec, J.-F. Lambert and C. Louis, *J. Phys. Chem. B*, 2002, **106**, 2277.
19 H. Yue, Y. Zhao, S. Zhao, B. Wang, X. Ma and J. Gong, *Nat. Commun.*, 2013, **4**, 2339.
20 W. Di, J. Cheng, S. Tian, J. Li, J. Chen and Q. Sun, *Appl. Catal., A*, 2016, **510**, 244.
21 M. A. Sánchez, G. C. Torres, V. A. Mazzieri and C. L. Pieck, *J. Chem. Technol. Biotechnol.*, 2017, **92**, 27.
22 R. Lu, D. Mao, J. Yu and Q. Guo, *Ind. Eng. Chem*., 2015, **25**, 338.

Received: 9th February 2024; Com. 24/7392